반도체및디스플레이장비학회지 제3권 제2호(2004년 6월)
Journal of the Semiconductor & Display Equipment Technology, Vol. 3, No. 2. June 2004.

Error Compensation of Laser Interferometer for Measuring Displacement Using the Kalman Filter

Tong Jin Park[†], Yong Woo Lee*, Young Yong Wang, Chang Soo Han***
Nak Ku Lee****, Hyung Wok Lee****, Tae Hoon Choi****, and Kyung Whan Na****

[†]Prec. Mechanical Engineering, Hanyang University, *LG Production Engineering Research Center,
Korean Railroad, ***Mechanical Engineering , Hanyang University, ** KITECH

ABSTRACT

This paper proposes a robust discrete time Kalman filter (RDKF) for the dynamic compensation of nonlinearity in a homodyne laser interferometer for high-precision displacement measurement and in real-time. The interferometer system is modeled to reduce the calculation of the estimator. A regulator is applied to improve the robustness of the system. An estimator based on dynamic modeling and a zero regulator of the system was designed by the authors of this study. For real measurement, the experimental results show that the proposed interferometer system can be applied to high precision displacement measurement in real-time.

Key Words : Interferometer, Kalman Filter, Error Model, Real Time Error Compensation, Bending Test

1. Introduction

The laser interferometers are used for the precision displacement measurement offering both a wide measuring range from below 1 mm to a few 10 m and theoretically unlimited resolution. For this reason, displacement measurement interferometers(DMI) are used extensively in precision position measuring. System measurement accuracy, however, is mainly limited both by nonlinearity from polarization mixing and by error from the installing environment of the interferometer. In general, nonlinear measurement error factors include unequal gains and zero offsets of the detectors, phase quadrature error, alignment error and polarization mixing in the optical system[1-4]. The error factors originating in the environment include, but are not limited to, vibration, temperature variation, and air turbulence[1]. Generally, the error from the nonlinearity is more than some ten nanometers in the case of the heterodyne interferometer. In the case of the homodyne, the error is less than any nanometer when it is well-aligned[2][5]. This nonlinearity was first described for heterodyne systems by Bobroff[1].

In addition, the elliptical fitting method by the least square algorithm has been investigated using a single wavelength in the homodyne interferometer[5-9]. The elliptical fitting method requires many time-consuming procedures, so this method cannot be used for real-time measurement[5]. Kim and et al. studied the least square method applied to the accelerated phase-measuring algorithm[3]. Li, Herrmann and Pohlenz proposed the correction of nonlinearity in a single-frequency interferometer based on a neural network model[4]. The neural network modeling method, however, is more suitable for off-line work due to its computational complexity. Eom and et al. suggest an automatic system for real-time correction in the homodyne laser interferometer.

This system consists of an electronic circuit for automatically optimizing the phase-quadrature signals and two commercial data acquisition boards[5]. As the studies in [3-5] focus on the nonlinearity of the laser interferometer, real errors such as light source, vibration, temperature and others, should be considered in real-time measurement. This paper proposes that precision displacement measurement with nanometer accuracy reduced errors. As well, it presents the design of

[†]E-mail : djpark@ihanyang.ac.kr

a real-time estimator.

The Kalman filter is the representative estimator for existing error. Zhu and Soh investigated correction and estimation of the system regarding nonlinearities as disturbances[11]. Waller and Saxen proved that the estimation cost is lower based on the more precise system modeling[12].

The goal of this paper is to improve accuracy of the laser interferometer with nanometer accuracy applied to robust estimator in real time. In particular, we are modeling a laser interferometer. The errors of the system divide from disturbance by nonlinearity, in laser source as well as in vibration and temperature. Applied to the robust Kalman filter minimized the error in the system, in this case we were able to demonstrate high precision DMI.

Section 2 describes the dynamic modeling of the system while section 3 describes the design for the estimator in real time. Section 4 describes performance validation of the estimator and section 5 describes experiment results and consideration on real measurement. Finally, section 6 presents the conclusions of this paper.

2. Laser Interferometer modeling

Fig. 1 shows the laser interferometer optical system and signal flow. As shown in Fig. 1, the system consists of both high precision DMI and the signal detected by four photo-detectors. A vertical polarized HeNe laser at the wavelength 0.6329 μm is used as a beam source. In the path of the laser beam, a half-wave plate first rotates the polarization from vertical to approximately 45°, so that the polarizing beam splitter that follows can split the beam into two nearly equal components, one directed to the reference retro-reflector and the other to the object retro-reflector, which is fixed on a flexure micro-stage being actuated by a PZT. Both beams from two retro-reflectors travel back and have interference at the polarizing beam-splitter. The non-polarizing beam splitter divides the beam into two nearly equal components. One of these components is sent directly to a polarizing beam splitter, which produces a pair of interference patterns in phase opposition. The other component is made to pass through a quarter-wave plate at 45°, so that an extra λ/4 delay is added to the optical path difference. The final polarizing beam splitter then produces a pair of patterns in phase opposition, but with λ/2 phase lag with respect to the previous ones. Overall, four quadrature signals are available at the photo-detectors. The interference signals detected by four photo-detectors have the phases of 0°, 90°, 180° and 270°, respectively. The system modeling is derived from the system signal output.

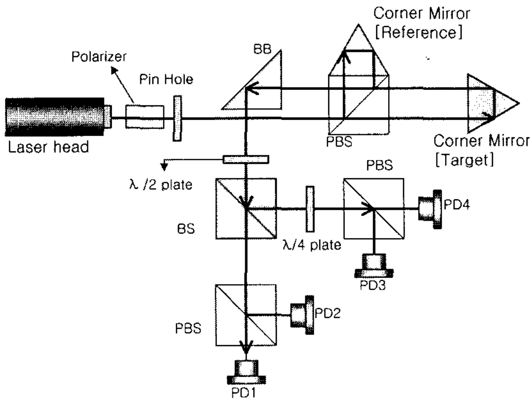

Fig. 1. Schematic of the displacement measurement interferometer.

Laser interferometer, according to variation of the beam intensity, can be regarded as sinusoidal functions representing a relationship between input and output of the signal. Equations (1) and (2) are ideal modeling equations for an interferometer.

$$I_x = I_1 - I_2 = \cos\phi \tag{1}$$

$$I_y = I_3 - I_4 = \sin\phi \tag{2}$$

where $\phi = \omega t$, ω is a phase frequency and t is time.

Two signals I_x, I_y with a phase difference of 90° are obtained by subtracting the signal with phase of 180°(I_2) from the signal of 0° (I_1) and the signal with phase 270°(I_3) from the signal of 90°(I_4)[4][5]. In an ideal case, assuming no system modeling error and no sensor noises, the laser interferometer modeling equation can be converted by Laplace transform as in the following equations. I_1, I_2, I_3, I_4 are the output signal of photo detectors(PD1, PD2, PD3, PD4 in Fig.1)

$$I_1(s) = \frac{y_1(s)}{u_1(s)} = \frac{s/2}{s^2 + \omega^2} \tag{3}$$

$$I_2(s) = \frac{y_2(s)}{u_2(s)} = \frac{-s/2}{s^2+\omega^2} \quad (4)$$

$$I_3(s) = \frac{y_3(s)}{u_3(s)} = \frac{\omega/2}{s^2+\omega^2} \quad (5)$$

$$I_4(s) = \frac{y_4(s)}{u_4(s)} = \frac{-\omega/2}{s^2+\omega^2} \quad (6)$$

Input signals, u_1, u_2, u_3 and u_4 are the power of a laser and Output signals, y_1, y_2, y_3 and y_4 are laser phase measurements with voltage dimensions. The state space equation for the laser interferometer system is as follows:

$$\begin{aligned} \dot{x}_i &= A_i x_i + B_i u_i \\ y_i &= C_i x_i \end{aligned} \quad , i=1\sim4 \quad (7)$$

where

$$A_1 = A_2 = A_3 = A_4 = \begin{bmatrix} 0 & \omega^2 \\ -1 & 0 \end{bmatrix}$$

$$B_1 = B_2 = B_3 = B_4 = \begin{bmatrix} 1 \\ 0 \end{bmatrix}$$

$C_1 = [1/2 \;\; 0]$, $C_2 = [-1/2 \;\; 0]$,
$C_3 = [0 \;\; -\omega/2]$, $C_4 = [0 \;\; \omega/2]$

Real signal modeling can be regarded with adding system modeling error and sensor noises.

Fig. 2 shows the signal output from the laser interferometer as stated in Fig. 1.

Equation (8) and (9) are modeling equations which consider system modeling errors and sensor noises.

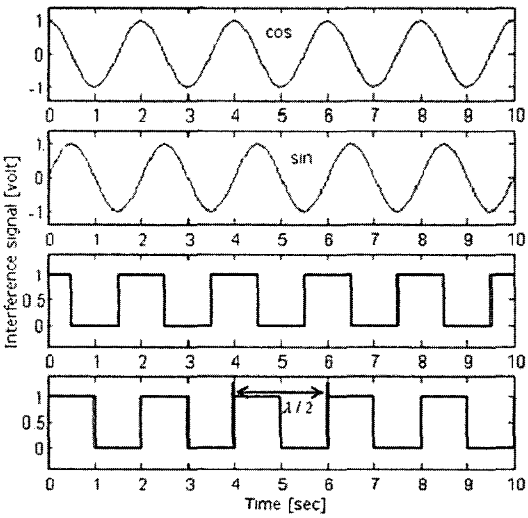

Fig. 2. Signal output plot of I_x, I_y in interferometer.

$$I_{x'} = I_{x_0} + a\cos(\phi - \psi) \quad (8)$$

$$I_{y'} = I_{y_0} + b\cos(\phi - \psi) \quad (9)$$

Where I_x and I_y are DC offsets. a and b are amplitude of the interference fringe, is the phase quadrature error of the DMI. Table 1 shows the error modeling factors of the laser interferometer system according to error values in equation (8) and (9).

Table 1. Value of the system and measurement noise.

Error value	Error factor
h, k	imperfection of the electronic circuit
a, b	laser power drift
ψ_x, ψ_y	polarization mixing effect

Using Laplace transform, equation (8) and (9) can be converted as follows:

$$I_{x'}(S) = \frac{as}{s^2+(\omega-\varepsilon)^2} + I_{x_0}(s) \quad (10)$$

$$I_{y'}(S) = \frac{b(\omega-\varepsilon)}{s^2+(\omega-\varepsilon)^2} + I_{y_0}(s) \quad (11)$$

where, we assume $y = \varepsilon t$, ε, is phase frequency error of fringe. Equation (12) is the state space equation for equation (8) and (9)

$$\begin{aligned} \dot{x}_i &= (A_i + \Delta A_i)x_i + B_i u_i + w_i \\ y_i &= C_i x_i + D_i u_i \end{aligned} \quad , i=1\sim4 \quad (12)$$

where,

$$A_1 = A_2 = A_3 = A_4 = \begin{bmatrix} 0 & -1 \\ \omega^2 & 0 \end{bmatrix}$$

$$\Delta A_1 = \Delta A_2 = \begin{bmatrix} 0 & 0 \\ 0 & 0 \end{bmatrix}$$

$$\Delta A_3 = \Delta A_4 = \begin{bmatrix} 0 & 0 \\ \psi^2 - 2\omega\psi & 0 \end{bmatrix}$$

$$B_1 = B_2 = B_3 = B_4 = \begin{bmatrix} 1 \\ 0 \end{bmatrix}$$

$$w_1 = \begin{bmatrix} 0 \\ I_{x_{01}} \end{bmatrix}, w_2 = \begin{bmatrix} 0 \\ I_{x_{02}} \end{bmatrix}, w_3 = \begin{bmatrix} 0 \\ I_{y_{01}} \end{bmatrix}, w_4 = \begin{bmatrix} 0 \\ I_{y_{02}} \end{bmatrix}$$

$C_1 = [a/2 \;\; 0]$, $C_2 = [-a/2 \;\; 0]$
$C_3 = [0 \;\; b\omega/2]$, $C_4 = [0 \;\; -b\omega/2]$
$D_1 = [0 \;\; 0]$, $D_2 = [0 \;\; 0]$
$D_3 = [0 \;\; -a\psi/2]$, $D_4 = [0 \;\; b\psi/2]$

PD sensor noises for I_1, I_2, I_3, *and* I_4 are independent. In addition, interaction between the laser interferometer system noise and photo sensors does not exist. Namely, noises in the laser interferometer can be regarded as uncorrelated. Assuming, therefore, that the average of offset error is zero, $w_i(t)$ and $D_i(t)$ can be modeled uncorrelated zero-mean Gaussian noise. The covariance of offset error can be expressed as

$$E\{w_{i,k} \cdot w_{i,s}\} = \begin{cases} Q(t) & if \quad k = s \\ 0 & otherwise \end{cases} \tag{13}$$

$$E\{D_{i,k} \cdot D_{i,s}\} = \begin{cases} R(t) & if \quad k = s \\ 0 & otherwise \end{cases} \tag{14}$$

3. Robust Discrete Time Kalman filter design

The Kalman filter is designed for estimating the system parameters based on the system modeling as described in section 2. In previous research, the system parameter can be only estimated in off-line data[3]. Fig. 3 shows the block diagram for designing the robust Kalman filter.

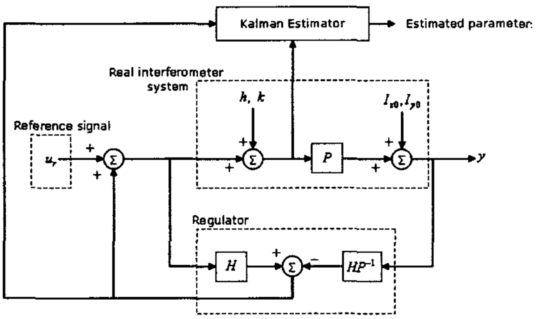

Fig. 3. Kalman Filter signal flow based on the modeling.

As the laser interferometer system is separated the reference system, A_i, and the system modelling errors, ΔA_i in eq(12), the parameters of the laser interferometer system can be estimated faster than the modelling of the black box system[13]. Real time measurement in the laser interferometer system is constructed by fast estimator. If the system modelling errors ΔA_i are at least bounded, and the system model is time-invariant and positive definite, the system parameters can be estimated. In addition, if the system model is attractive, the system estimator has a robustness to estimate system parameters even though the time-varying system[13]. A filter is applied to the system which is bounded and regulated to zero compensating robustness for ΔA. The robust estimator can be designed by correcting the system error clearly. As sampling rate is 10~100 [Hz], the filter is design for compensating ψ in this scope. Equation (15) is the filtering equation for compensating the system modeling error ΔA.

$$H(s) = K\frac{1 + \alpha Ts}{1 + Ts}, \ 1<\alpha \tag{15}$$

where, T is sampling time, K is a compensator gain.

As the compensator in equation (15) has the effect of increasing the system bandwidth, the noise in low-frequency does not affect the system. The Discrete Kalman filter is applied to the system which is compensated by the filter in equation (15). Equation (16) is the discrete modeling equation for the system in equation (12)

$$\begin{aligned} x_{i,k} &= A_{i,k-1}x_{i,k-1} + B_{i,k-1}u_{i,k-1} + w_{i,k-1} \\ z_{i,k} &= C_{i,k}x_{i,k} + D_{i,k}u_{i,k} \end{aligned} \tag{16}$$

Estimator equation applied to laser interferometer is as follows:

State estimate observational update, $\hat{x}_i$:

$$\hat{x}_{i,k} = x_{i,k-1} + \bar{K}_{i,k}[z_{i,k} - C_{i,k}\hat{x}_{i,k-1}] \tag{17}$$

Error covariance update, $\hat{P}_i$:

$$P_{i,k} = P_{i,k-1}[I - \bar{K}_{i,k}C_{i,k}] \tag{18}$$

Kalman gain matrix, $\bar{K}_k$:

$$\bar{K}_{i,k} = P_{i,k-1}C_{i,k}^T[C_{i,k}P_{i,k-1}C_{i,k}^T + R_{i,k}]^{-1} \tag{19}$$

The basic steps of the computational procedure for the Robust Discrete Kalman Filter (RDKF) are as follows:

1. Measure the system error signal, ψ;
2. Design the filter regulating for ΔA to zero;
3. Acquire the average and variance of the system offset error;
4. Acquire the average and variance of the sensor noises;

5. Compute $P_{i,k}$ using $P_{i,k-1}$, $\Phi_{i,k-1}$ and $Q_{i,k-1}$;
6. Compute $\bar{K}_{i,k}$ using $P_{i,k}$(computed in step 1), $C_{i,k}$ and $D_{i,k}$;
7. Compute values of $\hat{x}$ recursively using the computed values of $\bar{K}_{i,k}$ (from step 3), the given initial estimate $\hat{x}_{i,0}$ and the input data $z_{i,k}$.

Table 2. Value of the system and measurement noise.

Exp. Run No.	System noise	Measurement noise
10	−0.2564	1.3152
20	−0.2612	1.1354
30	−0.2831	1.4351
40	−0.2512	1.3032
Average	−0.2630	1.2972
Std. Deviation	0.0140	0.1232

4. RDKF performance evaluation

The system offset and measurement noise were acquired from many experiments in order to design robust estimator of the laser interferometer. Table 2 shows the resulting solutions of the measurement data

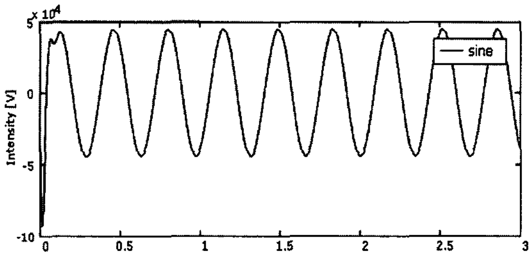

Fig. 4. Zero regulator performance simulation.

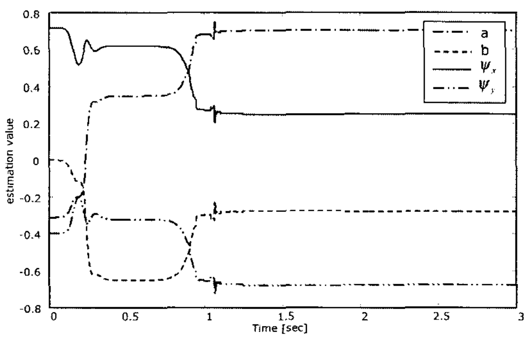

Fig. 5. System output result and parameter estimation in off-line simulation.

in real system. Through the results of many experiments, ψ has an average of -0.26 and measurement noise has an average of 1.3. The RDKF was designed as described in section 3 using the experimental data in Table 2. Fig. 3 shows the results of application of the filter to the system with filter regulating ΔA to zero.

Fig. 5 presents estimated parameters of the system using Kalman estimator applied to the zero-regulator and DTKF in off-line. Simulation results in Fig. 4 and Fig. 5 show the availability of the RDKF.

5. Experiment and results in real-time

Fig. 6 shows the configuration of laser interferometer used to implement accurate length measurements. The laser source is a HeNe laser of 633 nm wavelength. In this paper, the parameter estimations is constructed by applying the RDKF as designed in section 3 to the real laser interferometer system not using off-line estimation[3].

The precisely adjusted laser beam is then split by a polarizing beam splitter(PBS). One of the two beams with linear polarization is reflected by a retroreflector which is fixed on a moving stage. The stage, having a resolution <1 nm, 0.01% position Accuracy and 500 μm maximum moving range, is actuated by a piezo transducer. The other beam is reflected by a reference retroreflector. Both reflected beams are recombined in the PBS again and are sent directly to a polarizing beam splitter (PBS) to produce a pair of interference patterns. These interference patterns are received by four separated photo detectors, I_1, I_2, I_3 and I_4. The output signals of photo detectors with near quadrature can be formed as a rotated ellipse-like trajectory on an oscilloscope. A rotation of one-revolu-

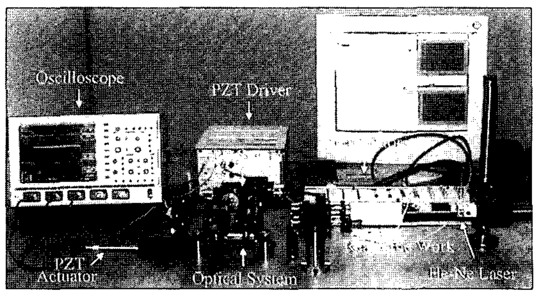

Fig. 6. Experimental Laser interferometer.

tion exactly corresponds to a $\lambda/2$ displacement and can be counted by using a counter. A Digital Signal Processor (DSP) is used for the RDKF. Sampling time is 1/1000 [sec]. Fig. 6 shows the results of the DMI applied the RDKF in real time.

Experimental results in Fig. 7 show the availability of the RDKF. Especially, the estimating time calculation can be reduced by using the system modeling in section 2 and the filter described in section 3 is available for system robustness.

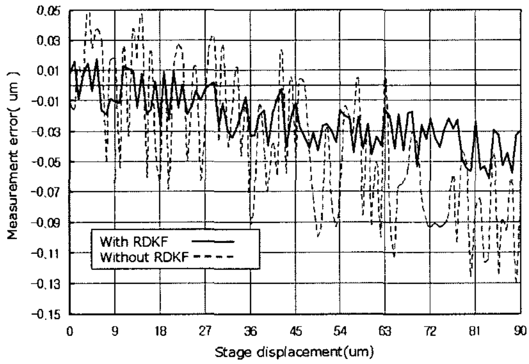

Fig. 7. Displacement measurement error with and Without RDKF.

6. Conclusions

The development of the high precision displacement measurement system using the robust real-time estimator was discussed in this paper. The conclusions of this paper are as follows:

(1) The system of laser interferometer was modeled to reduce the calculation time of Kalman filter.

(2) The robustness of the system estimator was considered using the filter which is regulating to zero for the system modeling error.

(3) With consideration of the characteristics of the system error and sensor noises, the discrete Kalman filter was designed.

(4) Applying the RDKF for the real system, the DMI with the estimator in real-time was constructed.

Acknowledgments

This work has been sponsored by MOCIE(Ministry of Commerce, Industry and Energy) of Korea as a part of the project of "Development of Micro optical and thermofluidic devices with high functionality".

References

1. Norman Bobroff, "Recent advances in displacement measuring interferometry", Meas. Sci. Technol. Vol. 4, 907-926 (1993).
2. Chunyong Yin, Gaoliang Dai and Zhixia Chao, "Determining the residual nonlinearity of a high-precision heterodyne interferometer", Opt. Eng., Vol. 38, pp.1361-1667 (1999).
3. Seung-Woo Kim, Min-Gu Kang and Geon-Soo Han, "Accelerated phase-measuring algorithm of least squares for phase-shifting interferometry", Opt. Eng., Vol. 36, pp.3101-3107 (1997).
4. Zhi Li, Konrad Herrmann and Frank Pohlenz, "A neural network approach to correcting nonlinearity in optical interferometers", Meas. Sci. Technol., Vol.14 pp.376-381 (2001).
5. TaeBong Eom, JongYun Kim and Kyuwon Jeong, "The dynamic compensation of nonlinearity in a homodyne laser interferometer", Meas. Sci. Technol. Vol.12, pp.1734-1738 (2001).
6. Chien-ming Wu, Ching-shen Su and Gwo-Sheng Peng, "Correction of nonlinearity in one-frequency optical interferometry Meas. Sci. Technol. Vol. 7, pp.520-524 (1996).
7. Chien-ming Wu and Ching-shen Su, "Nonlinearity in measurements of length by optical interferometry", Meas. Sci. Technol., Vol. 7, pp. 62-68 (1996).
8. Augustyn W and Davis P, "An analysis of polarization mixing errors in distance measuring interferometers", Vac. Sci. Technol., pp.2032-2038 (1990).
9. Heydemann LM. 1981 Determination and correction of quadrature fringe measurement errors in interferometers", Applied Opt., Vol. 20, pp. 3382-3386 (1981).
10. Dai Xiaoli and Seta Katuo, "High-accuracy absolute distance measurement by means of wavelength scanning heterodyne interferometry", Meas. Sci. Technol. Vol. 9, pp. 1031-1035 (1998).
11. Xing Zhu, Yeng Chai Soh and Lihua Xie, "Design and analysis of discrete-time robust Kalman filters Automatica, Vol. 38, pp.1069-1077 (2002).
12. Matias Waller and Henrik Saxén Estimating the degree of time variance in a parametric model Automatica, Vol. 36, pp. 619-625 (2000).
13. Karl Johan Astrom and Bjom Wittenmark, "Adaptive control : second edition", Addison-Wesley Publishing Company, (1995).